ICARUS 72, 394–410 (1987)

Variability of Ethane on Jupiter

THEODOR KOSTIUK,[1] FRED ESPENAK,[1] MICHAEL J. MUMMA,[1] AND DRAKE DEMING[1]

Planetary Systems Branch, Laboratory for Extraterrestrial Physics, NASA Goddard Space Flight Center, Greenbelt, Maryland 20771

AND DAVID ZIPOY[1]

Astronomy Program, University of Maryland, College Park, Maryland 20742

Received March 30, 1987; revised June 29, 1987

Abundances and spatial distributions of ethane in Jupiter's stratosphere were obtained from ultahigh-resolution ($\lambda/\Delta\lambda \sim 10^6$) spectra of individual C_2H_6 emission lines in the ν_9 band near 12 μm. The accuracy of the retrieved C_2H_6 mole fractions was evaluated in the context of varying stratospheric temperature profiles and C_2H_6 altitude distributions. A twofold uncertainty in the accuracy of the obtained abundances is possible. A mean equatorial value for the C_2H_6 mole fraction of $2.8 \pm 0.6 \times 10^{-6}$ was retrieved. Significant variability in the ethane line emission and retrieved mole fractions was found near the footprint of Io's flux tube and within the auroral regions. An increase in the ethane emission and abundance is obtained near the south polar region, relative to equatorial and northern latitudes. A significant decrease in ethane emission and abundance was observed in April 1983 near the known "hot spot" at 180° long (System III, 1965) and 60°N lat, where enhanced CH_4 and C_2H_2 emission was previously observed. We suggest that these observed phenomena are caused by a modification of local stratospheric chemistry, possibly by higher order effects of charged particles precipitating along magnetic field lines.

INTRODUCTION

The composition of the upper atmosphere of Jupiter is determined by photochemical processes of constituent hydrocarbons. Hydrocarbon chemistry on Jupiter has been studied theoretically by Strobel (1974), Yung and Strobel (1980), Gladstone (1983), M. Allen (1986, private communication, Jet Propulsion Laboratory, California Institute of Technology, Pasadena), and Atreya (1986). Ground-based (cf. Ridgway, 1974, Combes *et al.* 1974, Tokunaga *et al.* 1976, Kostiuk *et al.* 1983, Noll *et al.* 1986, Atreya 1986) and spacecraft (cf. Hanel *et al.* 1979a,b, Atreya *et al.* 1981, Kim *et al.* 1985, Atreya 1986) measurements in the ultraviolet and infrared spectral region have also been made on molecular spectra of various hydrocarbons in the Jovian stratosphere. These allowed retrieval of molecular abundances and atmospheric temperatures and provided a test for the existing atmospheric models. The determination of altitude and spatial distributions as well as relative abundances of the constituent molecules is particularly important because it can permit the extension of these photochemical models to multiple dimensions. Spatial distributions of Jovian stratospheric emission can also reveal local physical phenomena such as UV auroral effects in the polar regions (Clarke *et al.*

[1] Guest investigator, National Solar Observatory, a division of the National Optical Astronomy Observatories, which is operated by the Association of Universities for Research in Astronomy, under contract with the National Science Foundation.

0019-1035/87 $3.00

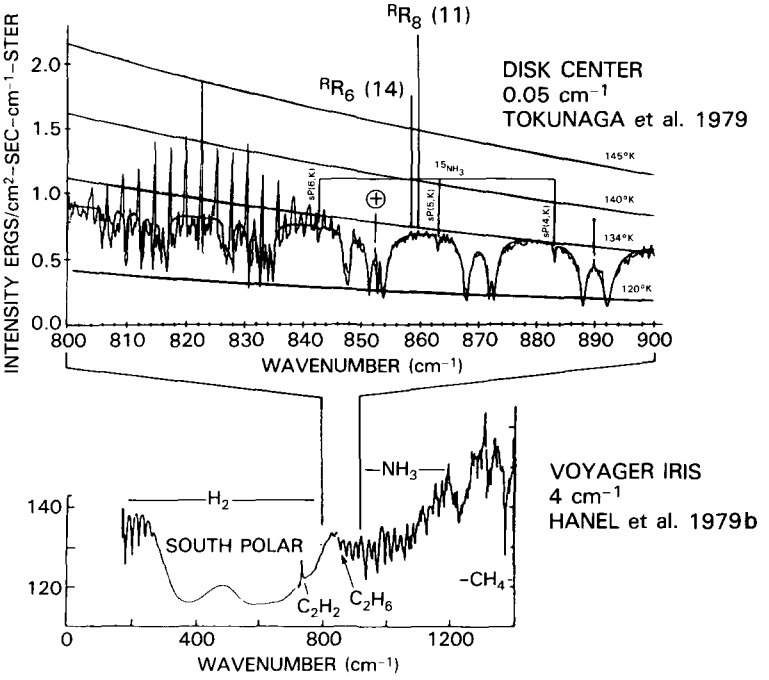

FIG. 1. The location of the RR(6, 14) and RR(8, 11) C_2H_6 lines in the band spectra measured by Voyager IRIS and ground-based Fourier transform spectroscopy. Even at 0.05 cm^{-1} resolution the lines are barely identifiable, with peak temperatures comparable to that of the continuum.

1980) and infrared hot spots with enhanced emission from CH_4 (Caldwell *et al.* 1980) and C_2H_2 (Drossart *et al.* 1986).

Ethane in Jupiter's south polar region as measured by the Voyager 1 infrared interferometer spectrometer, IRIS (Hanel *et al.* 1979b), at 4 cm^{-1} resolution appears as a broad feature near 820 cm^{-1} (Fig. 1). The broad fundamental band is composed of a series of unresolved subbranches as shown in ground-based spectra obtained by Tokunaga *et al.* (1979) at 0.05 cm^{-1} resolution (Fig. 1). These spectra directly probe only regions of pressures greater than 30 mbar. To obtain direct information on higher Jovian altitudes, the individual lines which make up the subbranches must be measured, requiring resolving powers $>10^5$.

We report here abundances and spatial distributions (vertical and horizontal) of C_2H_6 in Jupiter's stratosphere, obtained from ultrahigh-resolution ($\lambda/\Delta\lambda \sim 10^6$) spectra of individual ethane emission lines in the ν_9 band near 12 μm. Initial results of such measurements in the Jovian south polar region were reported by Kostiuk *et al.* (1983). The diffraction-limited spatial resolution of the heterodyne technique (~2 arcsec FWHM) permitted spatial mapping of the planet and the study of the localized "hot-spot" region near the north pole of Jupiter (Caldwell *et al.* 1980). The measurements were made in 1982 and 1983 using the Goddard Space Flight Center infrared heterodyne spectrometer (Kostiuk and Mumma 1983) at the McMath solar telescope at Kitt Peak National Observatory.

MEASUREMENT AND ANALYSIS

Although several C_2H_6 lines in the ν_9 band were measured, two lines were chosen as probes of the Jovian stratosphere, the RR, $K = 6$, $J = 14$ line and the RR, $K = 8$, $J = 11$ line. Both lines are doublets

TABLE I

Line[a]	K	J	σ	ν_{rest} (cm^{-1})	S (296°K) (cm^{-2} atm^{-1})	E'' (cm^{-1})
RR	6	14	0	858.10996	0.0123	211.5
RR	6	14	2	858.10651	0.0062	211.5
PR	1	29	1	858.09157	0.0026	578.9
PR	1	29	3	858.0829	0.0006	578.9
RR	8	11	0	859.78606	0.0034	216.0
RR	8	11	2	859.78340	0.0138	216.0
QQ[b]	10	12	2	859.7440	0.0020	360.0

[a] All lines are in the ν_9 band unless otherwise indicated.
[b] $\nu_9 + \nu_4 - \nu_4$ band.

formed by torsional splitting with a separation of $\sim 3 \times 10^{-3}$ cm^{-1} (Susskind *et al.* 1982). Line rest frequencies (ν_{rest}) and absolute intensities at 296°K of these doublets were taken from Daunt *et al.* (1984) and are given in Table I. The lower state energies E'' used to scale line intensities to Jovian temperatures are also listed. These lines were chosen for their favorable placement in the instrumental bandpass and their relatively high intensities. The positions of these lines in the band spectra are shown in Fig. 1; however, intensity dilution at 0.05 cm^{-1} reduces their measured line intensities to nearly the continuum level.

The fully resolved Jovian spectrum near 859.8 cm^{-1}, modeled for 60° zenith angle and an ethane mole fraction of 4.5×10^{-6}, is shown in Fig. 2. Several ν_9 lines are seen with a weaker $\nu_9 + \nu_4 - \nu_4$ QQ(10, 12, 2) hot-band transition A (W. Blass 1986, private communication, University of Tennessee, Knoxville) near the target RR(8, 11) line. Note that the strong line intensities are well above the continuum level. The position of the P8 transition of the $^{14}C^{16}O_2$ laser local oscillator, LO (solid line), and the ±0.0533 (±1.6 GHz) instrumental bandwidth (dashed lines) were shifted relative to the

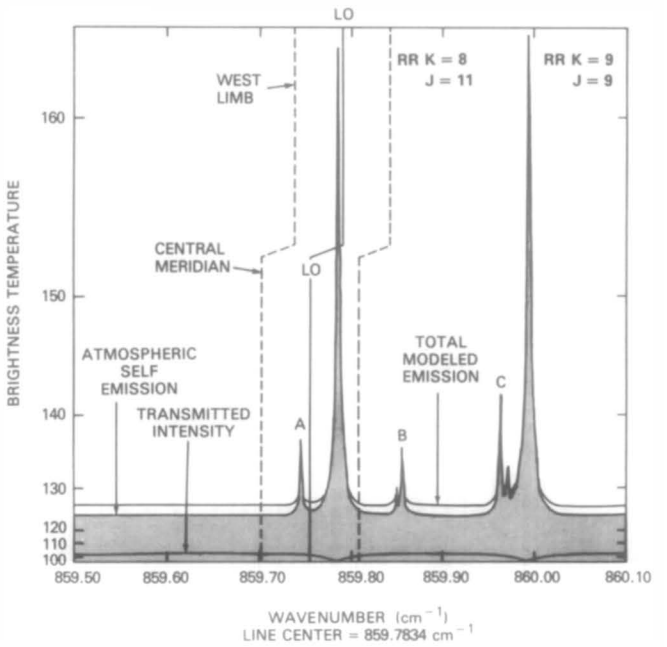

FIG. 2. The fully resolved Jovian spectrum near 859.8 cm^{-1} modeled for a viewing angle of 60°. The position of the laser local oscillator (LO) is shown for observations on the central meridian and on the west limb. For the limb observation the ethane spectrum is shifted 970 MHz (0.0323 cm^{-1}) to lower frequencies relative to the LO frequency by Jovian rotation. The broken lines define the instrumental bandwidth of ±0.0533 cm^{-1} about the LO. Line A is the QQ(10, 12, 2) line in the $\nu_9 + \nu_4 - \nu_4$ band. Lines B (RR(1, 26, 1)) and C (RR(2, 24, 2)) are in the ν_9 band (see Daunt *et al.* 1984). The C_2H_6 mole fraction used was 4.5×10^{-6}.

C_2H_6 rest frequency scale by an amount equal to the Doppler shift due to the Jovian geocentric velocity for April 8, 1982 of −9.8 km/sec (~840 MHz). For observations on the west limb Jovian rotation shifts the C_2H_6 spectrum by ~970 MHz to lower frequencies. The instrumental bandwidth and the laser line, as they would appear relative to the C_2H_6 rest frequency scale for this observing geometry, are also shown in Fig. 2. In both cases the RR(8, 11) ethane emission line is shifted well within the heterodyne bandwidth at the time of observation. The observed heterodyne spectrum will be the result of folding the spectrum about the local oscillator frequency, i.e., a double sideband spectrum (see Kostiuk *et al.* 1983, Kostiuk and Mumma 1983, Mumma *et al.* 1978).

Figure 2 also illustrates the components which make up the expected observed spectrum: the intensity transmitted through the atmosphere and the self-emission of the atmospheric layers. The sum of the two contributions (total modeled emission) is the spectrum which is used to fit our observations. This modeled spectrum was calculated by a solution of the radiative transfer equation using an atmosphere consisting of 34 layers extending from the ~700- to the ~0.14-mbar pressure level. It includes the upper troposphere, tropopause, and stratosphere of Jupiter. This encompasses the region where the contribution functions for the ethane line are significant (between 0 and 500 MHz from line center). The Jovian atmospheric model shown in Fig. 3 and a Voyager 2 temperature profile (Hanel *et al.* 1979a, J. Pirraglia 1984, private communication, NASA/Goddard Space Flight Center, Greenbelt, MD) for a latitude comparable to that of the observation was used. A constant mole fraction of C_2H_6 was assumed at altitudes above a cutoff pressure of 100 mbar (Fig. 3). The total measured continuum was assumed to be mostly due to the opacity of H_2 comprising 89% of the atmosphere and to NH_3 at a constant mole fraction of 2×10^{-4} between 150 and ~600 mbar (the cloud tops).

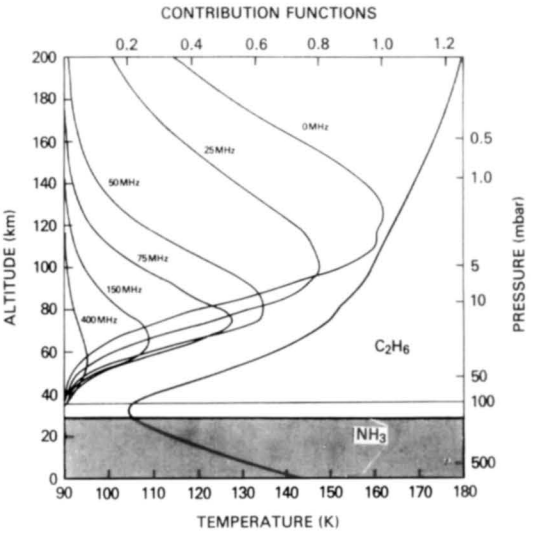

FIG. 3. The Jovian atmospheric model used in the analysis of the RR(8, 11) line including the south polar temperature profile and the contribution functions at various frequency offsets from line center.

The same line measured on Jupiter in 25 min of integration is shown in Fig. 4. The observed intensity converted to single sideband brightness temperature is plotted versus frequency over the 1600-MHz receiver bandwidth about the laser local oscillator (LO) transition. In this observation the absolute frequency of the Jovian ethane line is higher than that of the laser. The zero frequency value is arbitrarily set on the center of the stronger component of the emission doublet. The spectral resolution (each step in the histogram) is 25 MHz (0.00083 cm^{-1}) and is determined by the width of the RF filters in the filter bank (cf. Kostiuk and Mumma 1983). The fully resolved modeled spectrum is shown by the dashed curve. Note the expected doublet structure for the line and the weaker hot band transition A folded about the LO position to within 600 MHz of the doublet. The retrieved C_2H_6 mole fraction for this measurement near the Jovian south pole was 4.8×10^{-6}.

This modeled spectrum was calculated as described previously using the line intensities given in Table I, appropriately scaled to

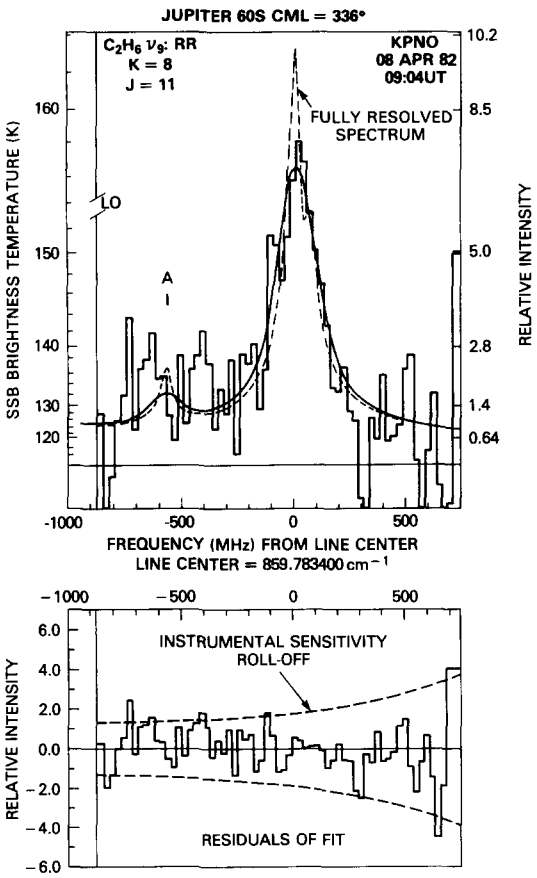

FIG. 4. The C_2H_6 RR(8, 11) line measured on Jupiter at 25 MHz resolution (histogram), the fully resolved modeled spectrum (dashed curve), and the rotationally broadened line (solid curve) which is fit to the data are shown plotted as single sideband brightness temperature versus frequency from the center of the stronger line in the doublet. The residuals of fit and the instrumental sensitivity roll-off, which is responsible for increasing noise level on the data as the frequency from the LO position is increased, are also shown.

Jovian atmospheric temperatures. An improved temperature-dependent pressure-broadening coefficient for C_2H_6 on H_2 of $\gamma_{HWHM} = 31.03T^{-1.02}$ cm^{-1}/atm, based on low-temperature laboratory measurements of Hillman *et al.* (1985), was also used. The calculated fully resolved lines are, however, broadened by ~100 MHz due to planetary rotation within our 2-arcsec field of view, making the doublet structure unobservable and the measured peak less bright. The solid curve in Fig. 4 represents the fully resolved lines convolved with an appropriate rotational broadening function defined by the beamwidth. It is this solid curve which is fit to our data by iterating on the C_2H_6 mole fraction. The residuals of the fit are shown in Fig. 4 along with the instrumental sensitivity roll-off. This sensitivity roll-off is responsible for an increasing noise level on the data as the absolute frequency difference from the LO transition is increased. The high spectral resolution permits direct sounding of stratospheric regions of pressures as low as ~1 mbar, as illustrated by the contribution functions for the fitted RR(8, 11) line in Fig. 3. This method of analysis and the atmospheric model are also described in Kostiuk *et al.* (1983).

The intensity (brightness temperature) calibration was done by comparison to measurements on the Moon and on a calibrated blackbody source. Measurements on a known point on the limb of the Moon were made at varying air mass over the night of the Jupiter observations. Lunar measurements were then scaled to the air mass of each Jovian measurement. Using tabulated lunar temperatures (Montgomery *et al.* 1966) and ratioing the Jupiter to Moon measurements removed any telluric contributions and established the brightness temperature scale. Similar calibration was done against a stable blackbody reference in our spectrometer. This was possible since Earth's atmospheric contributions are small at these wavelengths and the optical losses of system elements (including the telescope) are known. Results from the two calibration methods were in excellent agreement ($\lesssim$3°K). Taking into account this relative uncertainty and the estimated uncertainty in the knowledge of lunar temperature, an absolute error in our temperature scale of less than ±5°K was established.

Figure 5 illustrates a measurement on the RR(6, 14) line, the calculated fully resolved spectrum, and the rotationally broadened best-fit spectrum. The doublet structure is

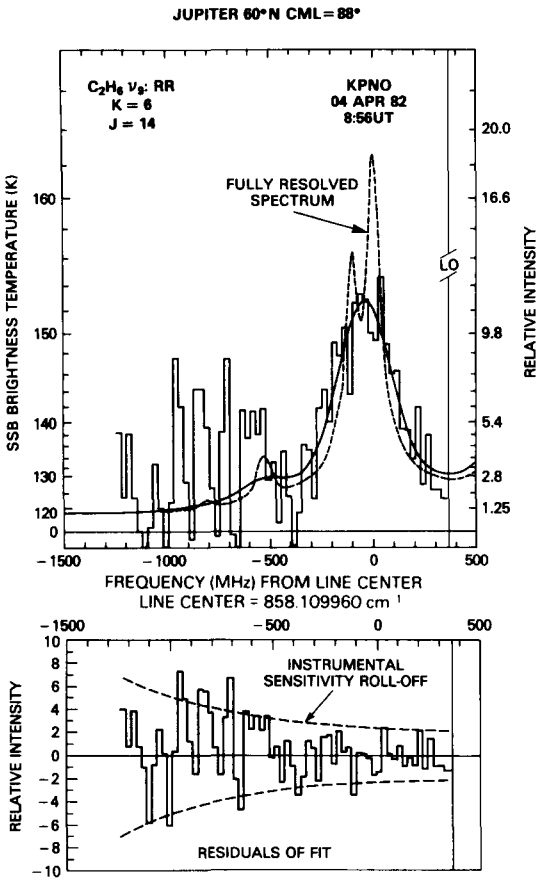

FIG. 5. The measured RR(6, 14) line, the modeled fully resolved spectrum, the best-fit spectrum (including rotational broadening), and the residuals of fit and instrumental sensitivity roll-off are shown (see Fig. 4 caption).

more prominent in this line due to a greater torsional splitting and higher relative intensity of the weaker doublet component. Note also the two weak transitions obtained in the modeled spectrum. Here again, the residuals and instrumental roll-off are presented. The higher noise on the data is clearly shown at the frequencies far from the laser transition. This C_2H_6 line appears at an absolute frequency below that of the laser LO.

This method of analysis and atmospheric model were used to study the spatial distribution of ethane on Jupiter and its variability in the north polar region.

RESULTS AND DISCUSSION

Spatial Distribution

The geometry for the observations as well as actual data obtained at various positions on the planet are presented in Figs. 6 and 7. The 2-arcsec diameter (FWHM) instrumental field of view is shown on a planetary disk of ~40-arcsec diameter at the time of observation. Qualitatively the data behave as expected for a stratospheric constituent. The C_2H_6 emission line is much more pronounced near the planetary limbs where a greater stratospheric column is observed along our line of sight. As the observations approach disk center the measurement is of a thinner stratospheric layer and,

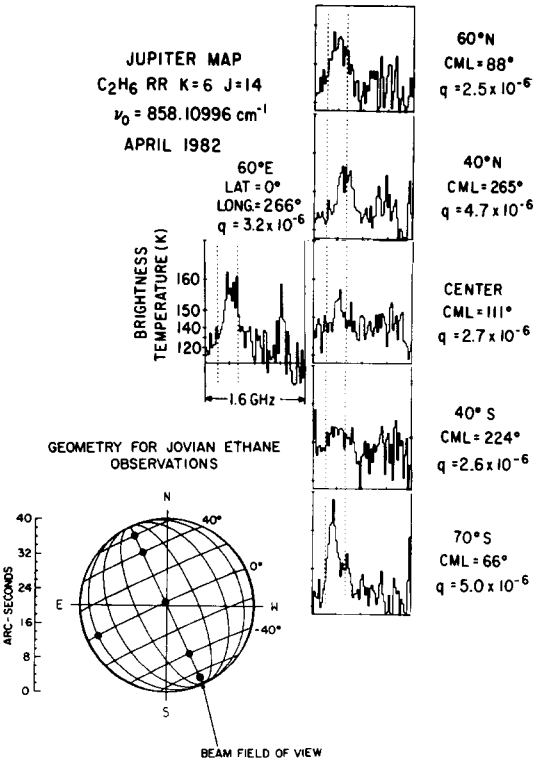

FIG. 6. Spatial map of Jupiter in the C_2H_6 RR(6, 14) line. The retrieved mole fractions at each position are given. The geometry of the observations is also shown with the 2-arcsec instrumental field of view on the 40-arcsec-diameter Jovian disk. Jovian rotation velocity Doppler shift permitted only the east limb to be measured using this ethane transition.

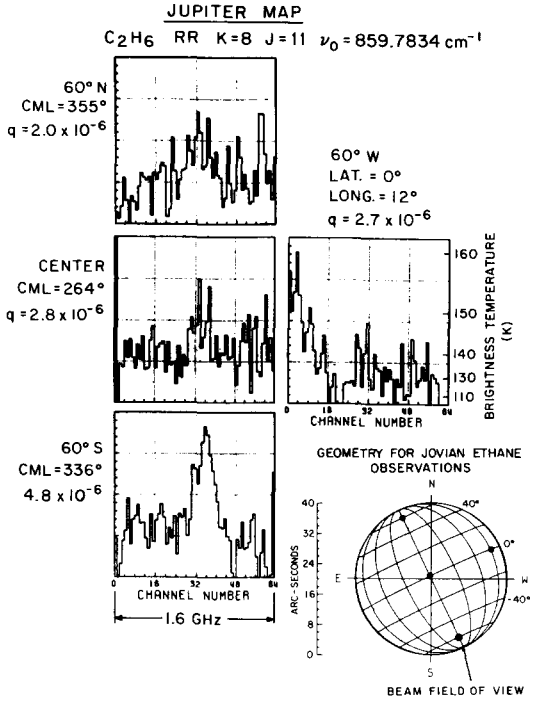

FIG. 7. Spatial map of Jupiter in the C_2H_6 RR(8, 11) line taken April 8, 1982. The instrumental field of view and the geometry of the observations are also given. This ethane line could be used to observe the west limb, but not the east limb, due to the Doppler shift in line frequency as a result of Jovian rotation.

thus, the emission-line intensity is reduced. The measured continuum, however, increases, indicating that we are probing deeper into the atmosphere below the tropopause where it is hotter. The retrieved C_2H_6 mole fractions are given for each measurement. Note that, with the exception of the 40° north measurement and the south polar region, the retrieved mole fractions are close to $\sim 3 \times 10^{-6}$. The south polar emission lines appear to be narrower and brigher compared to lines measured on the other limbs. This is consistent with the brighter retrieved C_2H_6 mole fractions of $\sim 5 \times 10^{-6}$.

Data displayed in Fig. 6 are of the RR(6, 14) line taken April 5, 1982, and those shown in Fig. 7 are of the RR(8, 11) line taken April 8, 1982. Measurements on both the east and west limbs were not possible using the same C_2H_6 transition, since the Doppler shift due to planetary rotation shifts the observed line out of the instrumental bandpass. Full coverage is possible with one line along the central meridian, where the rotational Doppler shift is zero. Results obtained along both N–S and E–W directions are consistent in both sets of measurements. The lower signal-to-noise ratio on the data in Fig. 7 is due to "wind shake" of the heliostat in the N–S direction during the measurements on April 8, 1982.

A summary of the results obtained from measurements during three observing periods, April 1982, May 1982, and April 1983, is given in Fig. 8. The coordinates of each observation are plotted on a latitude–longitude grid (System III, 1965). The retrieved mole fraction for the measurement is given at each plotted point. In the equatorial region the retrieved mole fractions are relatively constant with an average value of 2.8 $\pm$ 0.6 $\times$ 10^{-6}. One value was slightly higher

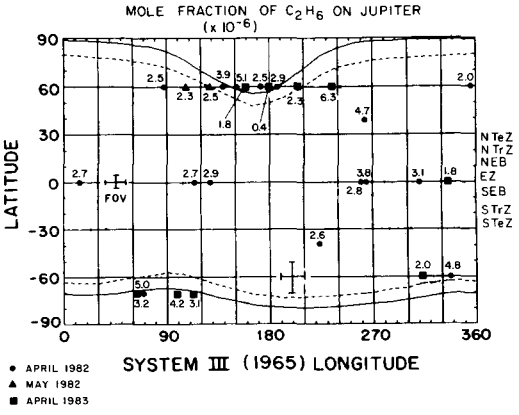

FIG. 8. Summary of the mole fractions obtained from our measurements during observing periods in April 1982, May 1982, and April 1983. The result of each observation is plotted at the appropriate beam coordinates on Jupiter on a latitude–longitude grid (System III, 1965). The extent of the field of view covered by each measurement (~25 min integration) is shown by the error bars at the equator and at 60° lat. The auroral oval is defined by the solid curves and the footprint of Io's flux tube is defined by the broken line (Connerney *et al.* 1981).

(3.8×10^{-6}), whereas a lower result of 1.8×10^{-6} was obtained from measurements taken during a different observing run. The mole fractions retrieved from our total data set remain close to the average equatorial value everywhere on the planet outside the auroral oval (Fig. 8, solid curve), and the footprint of Io's flux tube (Fig. 8, broken line) (Connerney *et al.* 1981). Greater variability of the retrieved C_2H_6 mole fractions is observed at these boundaries and inside the auroral region. Higher values ($\sim 5 \times 10^{-6}$) are obtained near these boundaries and, as will be discussed later, some very low values are found within the north auroral region. Due to the position of the Jovian rotation axis at the time of observation and the defined auroral regions, the instrumental field of view in the south polar measurements almost always included the auroral zone and flux-tube boundary. In those measurements the emission line and retrieved C_2H_6 mole fractions were found to be greater than elsewhere on the planet.

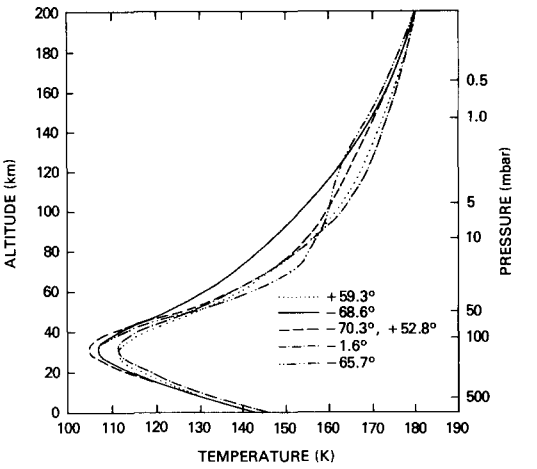

FIG. 9. Temperature profiles derived from Voyager IRIS data used to model our observations.

Measurement and Retrieval Uncertainities

The precision in the retrieval of C_2H_6 mole fractions for a given set of input parameters is about ±20%, determined primarily by the signal-to-noise ratio on the measurement. The accuracy of the retrieved values is, however, dependent on the accuracy of the input parameters. These parameters are the molecular line parameters for C_2H_6; the Jovian atmospheric model, including the temperature profile and the assumption of constant mixing ratio of C_2H_6 above the 100-mbar level; and the knowledge of the coordinates of the measurement on the planet.

The molecular line parameters are given in Table I. The line frequencies are accurate to ±0.001 cm^{-1}. This uncertainty permits unambiguous identification of the lines and does not affect the Jovian retrievals, since the modeled profile line center is fit to the center frequency of the measured line. A very precise ($1:10^7$) relative frequency scale is established by the heterodyne measurement (RF filters) and a highly accurate ($1:10^8$) absolute frequency is determined by the laser transition. The uncertainty in line intensities is ±10%, which translates into ~±10% error in the retrieved C_2H_6 mole fractions. The temperature-dependent pressure-broadening coefficient was measured specifically for this investigation (Hillman *et al.* 1985) and is an improvement over the previously used value (Kostiuk *et al.* 1983). It should contribute insignificant error in the present analysis.

The accuracy of the retrieved C_2H_6 abundance values is mostly dependent on the accuracy of the atmospheric model used, specifically the temperature profile and vertical ethane distribution. This can be illustrated by considering the effect of changes of the atmospheric model (Fig. 3) on the retrieved ethane abundance.

Sensitivity to changes in the temperature profile. In all the analyses we have used temperature profiles derived from Voyager IRIS data at latitudes corresponding closely to those of our heterodyne observations (Fig. 9). These profiles can vary considerably (~10°K) in the stratosphere over the planet, even at positions of nearly equal latitude. Fitting a given set of data using the two most extreme temperature profiles,

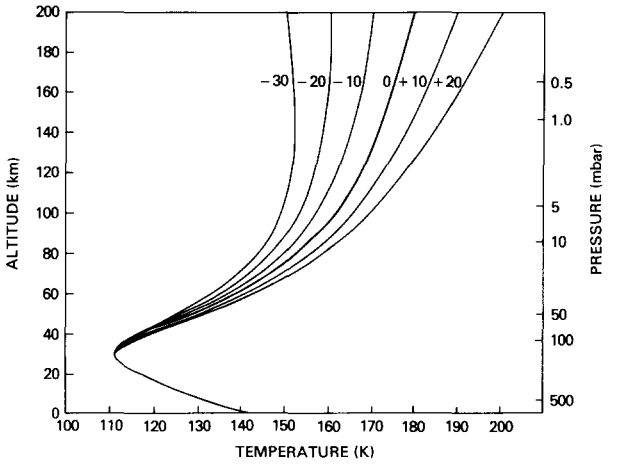

FIG. 10. A standard (+59.3°) temperature profile (0) varied by 10°K increments at the top of our model (0.14 mbar). The altitude scale is for the standard temperature profile (0). These profiles were used to investigate the sensitivity of Jovian ethane emission to changes in the stratospheric temperature (see text).

−68.6° and +59.3°, yields a twofold difference in the retrieved mole fraction. Due to the noise level of the data, no significant difference is observed between the two cases in the quality of the fits.

To test the ethane emission-line dependence on stratospheric temperature alone, line profiles were modeled starting with a fixed C_2H_6 mole fraction and a standard temperature profile. The stratospheric temperature was then varied. Figure 10 illustrates the profiles used. The temperature inversion point was fixed and the maximum incremental temperature change was at the top of our model (~0.14 mbar). Line profiles for the RR(6, 14) line calculated for varying statospheric temperatures (in 10°K increments at 0.14 mbar) are shown in Fig. 11a. An increase in stratospheric temperature of ~5°K at 2 mbar (~10°K at 0.14 mbar) would increase the line brightness temperature by ~5°K. This is about the uncertainty in our temperature calibration. Much greater increases in stratospheric temperature are, therefore, outside our experimental uncertainty. As we decrease the stratospheric temperature profile similar arguments hold and a ~10°K model top (5°K, 2 mbar) decrease is the maximum change consistent with this data set. Note that, in order for the line to be undetectable at our signal-to-noise ratio (and the fixed mole fraction) the stratospheric temperature at 2 mbar would have to be decreased by >20°K (−30°K in Fig. 11a, peak line brightness temperature ≲135°K; compare to the actual data plotted from Fig. 5).

Sensivitiy to change in C_2H_6 abundance and mixing profile. Figure 11b illustrates how the observed ethane line would change with changing C_2H_6 mole fraction for a given temperature profile. The mole fractions used in the modeled lines were varied from one-quarter to four times the value retrieved from the measured data in Fig. 5 (2.6×10^{-6}). The curves are labeled by the factors multiplying the standard mole fraction value. From Fig. 11b it is seen that a twofold change in C_2H_6 mole fraction would exceed our absolute uncertainty in the brightness temperature scale (~5°K).

Comparing peak brightness temperatures to those in Fig. 11a, a twofold decrease in C_2H_6 abundance is consistent with ~15°K maximum decrease in the upper stratospheric temperature profile (~8°K at 2

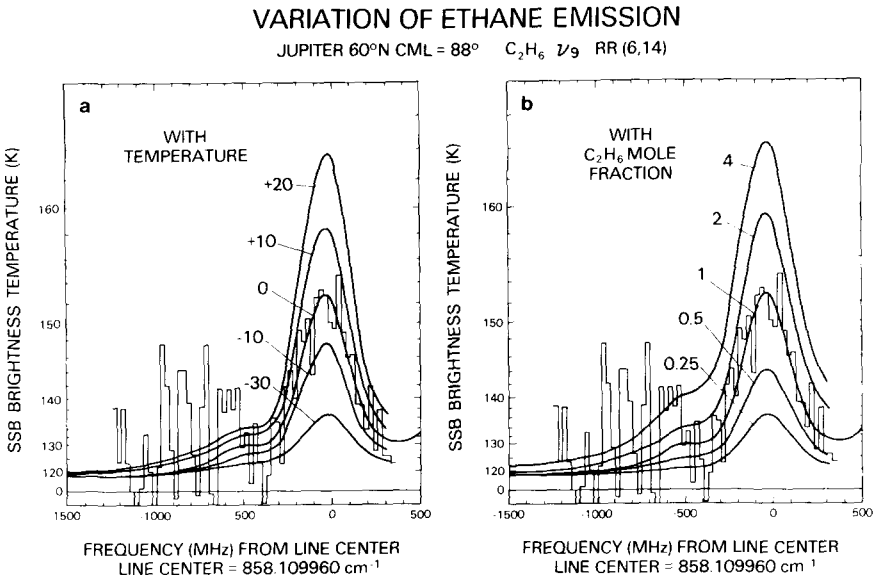

FIG. 11. (a) Stratospheric RR(6, 14) lines on Jupiter (60°N) as modeled using the temperature profiles of Fig. 10 and a constant C_2H_6 mole fraction of 2.6×10^{-6}. Each curve is labeled by the incremental temperature change at 0.14 mbar of the respective temperature profile. The measured data from Fig. 5 are also plotted for comparison. (b) Changes in the RR(6, 14) Jovian line profile (60°N) as a function of changing C_2H_6 mole fraction on Jupiter for a given temperature profile (+59.3°). The lines are labeled by factors multiplying the mole fraction value retrieved from observations, 2.6×10^{-6}. The measured data from Fig. 5 are also plotted for comparison.

mbar). For the given atmospheric model the retrieved C_2H_6 mole fraction would have to decrease by more than a factor of 4 to be undetectable at the noise level on the data (compare to data plotted from Fig. 5).

All data analysis and uncertainty considerations assume a constant mole fraction of C_2H_6 in the Jovian stratosphere (above the 100-mbar level). This assumption approximates existing photochemical models (Strobel 1974, Yung and Strobel 1980, Gladstone 1983). To investigate the changes in the retrieved C_2H_6 abundances that a nonconstant mixing profile would introduce, the RR(6, 14) line was fit using an altitude distribution model obtained by Allen (1986). The shape of his altitude distribution was preserved during our integration while the mole fraction value in each layer was varied. The resultant vertical distribution profile for our standard 59.3° temperature profile is shown in Fig. 12. The peak mole fraction is $\sim 3.5 \times 10^{-6}$ with a value of $\sim 1 \times 10^{-6}$ at 30 mbar. The total normal C_2H_6 column obtained was 0.52 cm-am compared

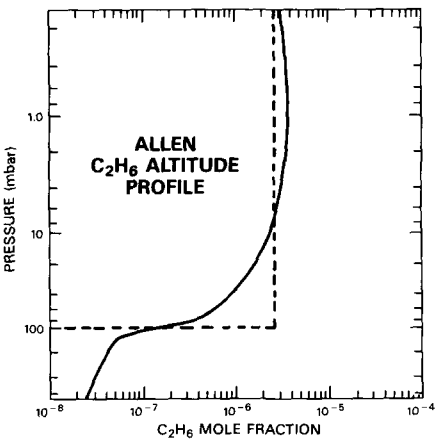

FIG. 12. The nonconstant altitude distribution model for Jovian ethane derived by Allen (1986) is given along with the constant stratospheric model used in the analysis of our data.

to 1.1 cm-am retrieved for the constant mixing profile. Due to the distribution of the contribution functions little information is obtained below the ~30-mbar level. Therefore, the differences between the retrieved total column density for the constant mixing profile and the variable vertical distribution mixing profile are not significant.

Contribution functions are dependent on the atmospheric temperature profile and viewing angle through the atmosphere as well as the ethane altitude distribution. In principle, measurements at various viewing angles can provide information on the altitude distribution, if the temperature profile is known. We investigated our ability to retrieve such information by comparing the altitudes at which our modeled contribution functions peak at the viewing angles of our observations (70, 60, 40, and 0°). For a given temperature profile and C_2H_6 mole fraction (2.6×10^{-6}), the pressure levels for the peaks of the 0-MHz contribution functions varied by a factor of ≤ 2 (e.g., 2–2.7 mbar for the +59.3° profile; 1.2–2.2 mbar for the colder −68.6° profile). The contribution functions are found to be not very sensitive to our range of viewing angles. Even at our high spatial resolution we cannot make measurements at a high enough viewing angle (true limb scanning) to obtain meaningful altitude shifts. Variation in the assumed mole fraction shifted the pressure levels of the contribution function peaks, at most, proportionally. These altitude variations are not significant since the implied changes in ethane abundance with altitude are comparable to or less than the accuracy in our retrieved C_2H_6 mole fractions. These contribution functions were for the fully resolved spectrum. If the rotational broadening function and noise on the data is folded in, even less altitude information is obtainable from our data. From these considerations we conclude that information on ethane altitude distribution on Jupiter cannot be extracted from our data.

All the "best-fit" line profiles obtained using various realistic atmospheric models in the analyses fit the measured data equally well. The retrieved ethane mole fractions, however, varied by as much as a factor of 2. We conclude that variations in the atmospheric models for C_2H_6 in the Jovian stratosphere can introduce an uncertainty of about a factor of 2 in the accuracy of the retrieved mole fraction and column density of ethane on Jupiter. Since the observed variability is within this range, we cannot exclude variation in stratospheric temperature, instead of C_2H_6 abundance changes, as an explanation for the observed variation.

Polar Variability

Caldwell *et al.* (1980) reported observing a hot-spot region within the auroral zone on Jupiter, near 60°N lat and 180° long, where enhanced emission of methane near 7.8 μm was observed. In order to study possible variability of the ethane emission within the north auroral region and to observe any changes near this polar hot-spot region we placed our 2-arcsec field of view on the Jovian central meridian at 60°N lat and allowed Jovian rotation to scan the auroral region as we continuously integrated on the

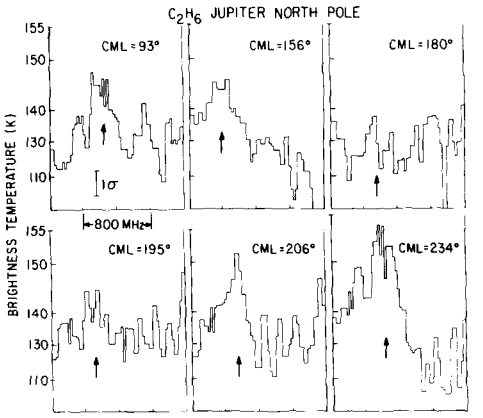

FIG. 13. Measurements of the RR(6, 14) line at 60°N latitude and central meridian longitude (CML) on Jupiter. Each spectrum represents about 18° in longitudinal coverage. The expected position of the ethane line is indicated by the arrow. The line disappears at CML = 180° (see text).

source. Data were taken in April and May 1982 and April 1983. Representative data taken in April 1983 are shown in Fig. 13. Each spectrum represents about 18° in longitudinal coverage on Jupiter. The brightness temperature versus IF frequency is displayed for various central meridian longitude (CML) positions. The predicted frequency locations of the C_2H_6 RR(6, 14) ethane emissions are indicated by the arrows. The 1-σ deviation per point is also shown. Qualitatively the emission appears to decrease from 93 to ~180° CML where it all but disappears. It then reappears and becomes more intense at 234° CML. Note that the continuum remains approximately constant at a brightness temperature of ~127°K.

The ethane mole fraction for each data set was retrieved as described previously. The resultant mole fractions are plotted versus the central meridian longitude in Fig. 14. The mole fraction value of $\sim 1.8 \times 10^{-6}$ is retrieved from 80 to 165° CML. Near 180° there is a sharp drop in the retrieved C_2H_6 abundance, consistent with the disappearance of the emission. The mole fraction again increases above 200° CML, rising to a somewhat larger value of 6×10^{-6} at 235° CML. The latitudinal range per point (due to integration time used per point) is shown in Fig. 14. From 160° on, the measurement was continuous and the points represent the centers of approximately half-hour stacks of data. The same temperature profile and atmospheric model were used at 60°N lat for analysis of all the data sets. The vertical error bars in Fig. 14 represent the precision of fit (~±20%). As discussed before, the accuracy of the retrieved values is limited to a factor of ~2. The rapid decrease and reemergence of the C_2H_6 emission near 180° CML and 60°N lat indicates a localized phenomena <4 arcsec in extent. The location and extent of this region are very similar to the hot-spot region reported by Caldwell *et al.* (1980), Kim *et al.* (1985), and Drossart *et al.* (1986) and subsequently

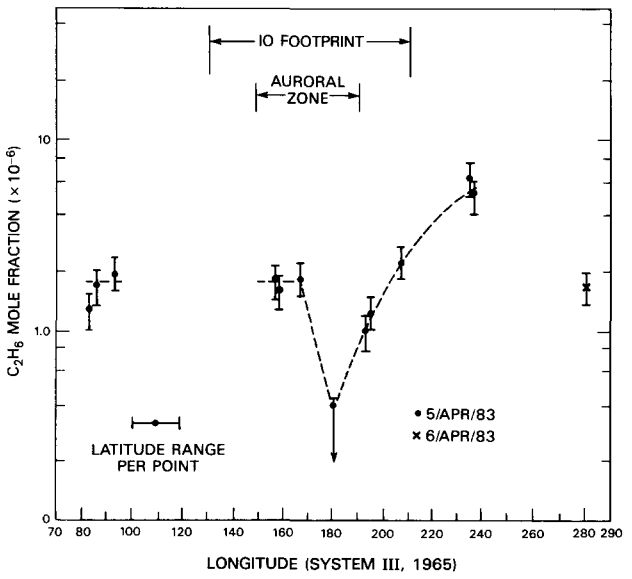

FIG. 14. The retrieved C_2H_6 mole fractions for north polar measurements (Fig. 13) as a function of longitude. The precision of the retrievals is given by the vertical error bars on each point. The error bars on the point at 180° indicate that even lower values of the mole fraction would fit the observation. The latitude range per point is also given. The decrease in ethane occurs well within the auroral zone and Io footprint.

mapped by Caldwell *et al.* (1987). In the 1982 measurements no large changes in the ethane emission were observed and the retrieved C_2H_6 mole fractions remained approximately constant ($2.9 \pm 0.8 \times 10^{-6}$) through longitudes of ~184°. A discussion of these results and of factors (including observational limitations) that were considered in interpreting these measurements is given below.

Field of view and pointing. An increase in the field of view on Jupiter or significant tracking errors on the planet could also affect the degree of measured ethane emission. Jovian rotational broadening (as was discussed previously) could broaden the emission line, thereby reducing its peak intensity. A diffraction limited field of view of 2.2 arcsec was used in the data analysis. The seeing or tracking errors would have to correspond to an effective spread of the field of view in the longitudinal direction of ~8 arcsec in order to reduce the emission peak below the noise level. Atmospheric seeing during the time of our observations was ≲2 arcsec as determined by visual monitoring of the source and checking the image quality of stellar sources. Tracking accuracy was checked by visual monitoring of the planet and by monitoring the velocity (frequency) shift of the lines in the measured data. These effects could not contribute to the reduction in the observed line emission. Absolute pointing, however, was determined from a visual image of Jupiter and could be responsible for latitudinal position uncertainties of ≲2 arcsec. This could cause us to miss the hot spot during some measurements, but could not, in itself, cause the disappearance of emission. This effect could also explain why no decrease of emission was observed in 1982.

Temperature vs abundance. Initially, Caldwell *et al.* (1980) speculated that charged particle–auroral effects were reponsible for the enhancements of the CH_4 emission at 7.8 μm in this region. Subsequently, an increase of about 10°K in stratospheric temperature was found to be consistent with increased CH_4 emission, but an increase in abundance was needed to explain observed increases in molecular band intensities of several species as derived from Voyager IRIS data (Kim *et al.* 1985). Enhancement of line intensities of C_2H_2 was also found by Drossart *et al.* (1986) at the hot-spot position. They attribute the enhancement to an increase in acetylene abundance, but do not rule out thermal or nonthermal effects. Drossart *et al.* (1985) noted an increase in C_2H_2 and C_2H_6 emissions at the hot spot, but a lesser change was observed in the C_2H_6 emission.

Neglecting changes in ethane abundance, a simple increase in stratospheric temperature would be observed by us as an increase in C_2H_6 line emission. As was illustrated in Fig. 11a, we would easily observe a 10°K brightening. In fact, we see no significant change in the emission line near the hot-spot region in April and May 1982, although our data did not cover longitudes greater than 184°. In April 1983 (Figs. 13 and 14) there appears to be a decrease in the ethane emission. The value of the retrieved mole fraction of C_2H_6 at 180° is at least five times lower than the global average. In fact, the value of 0.4×10^{-6} is an upper limit, since a 127°K continuum (no ethane emission) would fit the measured data in Fig. 13 equally well. From Fig. 11a, it would require a stratospheric temperature at 0.14 mbar more than 30°K (~20°K at 2 mbar) colder than our model to reduce the emission below the noise level. Both of these possible explanations are inconsistent with our knowledge of the Jovian atmosphere (cf. Hanel *et al.* 1979a,b, Gierasch *et al.* 1986).

Halthore *et al.* (1987) developed a thermal equilibrium model for the north polar hot spot based on Voyager IRIS data requiring upper stratospheric (pressures less than 1 mbar) temperatures between 220 and 250°K. Their model explains the enhanced 7.8 μm CH_4 emission. It also can be made consistent with the observed enhancement of 13.6 μm C_2H_2 emission, but requires that

the acetylene abundance be increased in the hot-spot region. Were ethane present in the abundances characteristic of regions outside the hot spot, its emission would also be enhanced. Since Halthore *et al.* (1987) do not observe a significant increase in ethane emission, they infer a depletion in the hot spot of ~80%. Although this model applies to altitudes above those we normally probe with our heterodyne measurements, 250°K temperatures at pressure levels of $\sim 10^{-2}$ mbar would still be observed by us as enhanced line emission.

In an attempt to relate the hot upper stratospheric model of Halthore *et al.* (1987) to our observed decrease of ethane emission, the ethane spectrum was modeled using an extreme temperature profile—isothermal at 110°K above the tropopause to 1 mbar (where most of the ethane is present) and hot, 200–250°K, at upper statospheric layers above the 1-mbar level (where the CH_4 emission is observed). Under these conditions the ethane line brightness temperature still exceeded 145°K with a 200°K upper stratospheric temperature and 165°K with a 250°K upper statospheric temperature. The lines were slightly narrower since pressure broadening was reduced and they would be easily observed with our instrument. Therefore, we see no evidence of such temperature distribution and there is no physical basis at this time to support such an exotic temperature profile on Jupiter.

Solar heating. Solar radiation incident on Jupiter shows a seasonal variation. This variation was calculated by Beebe *et al.* (1986), who show that at 60°N lat the incident solar radiation varies by +28 to −23% about the mean (±3°K in blackbody radiation temperature). At 60°S lat they show a variation of only ±10% (±1°K temperature variation). These variations have a period of 11.36 years and are small over the relatively short period when our observations were made. At the time of our observations the south pole received ~30% more solar radiation than the north. If the relevant Jovian atmospheric time constants are short compared to seasonal variations in incident solar radiation, solar heating can play a role in the thermal and chemical processes in the Jovian stratosphere, although direct heating to temperatures required to explain hot-spot phenomena is not likely. Solar heating may also be significant for dynamical processes (Beebe *et al.* 1986) which in turn may play a role in localized heating and the hydrocarbon chemistry.

Chemistry. It has been observed using Voyager IRIS data that the C_2H_2/C_2H_6 mole fraction ratio increases from south to north on Jupiter (Maguire *et al.* 1985). Since there is evidence for enhancement of C_2H_2 near the north pole (outside the polar hot spot) and, as discussed previously, a possible increase in C_2H_6 emission (mole fraction) in the south polar region, our results are consistant with the Voyager data. This fact and the north polar hot-spot results suggest that there is a changing chemistry in the Jovian stratosphere which, assuming a constant CH_4 abundance, preferentially forms C_2H_2 at the expense of C_2H_6. In the north polar hot spot this chemistry is further enhanced and, not only is more C_2H_2 present, but perhaps many minor constituent hydrocarbons are formed as well (cf. Kim *et al.* 1985). Ethane, however, may in fact be greatly reduced in this region. Temperature may indeed play a role in this chemistry and the source of heat may be a by-product of solar heating, auroral activity, or unique dynamics. The effect may also be altitude dependent. At 7.8 μm CH_4 is observed much higher in altitude (at pressures below 1 mbar) than is C_2H_6 (pressures >1 mbar).

Charged particle effects. The predominantly ultraviolet photochemistry of methane in the Jovian upper stratosphere may be affected by concentration of charged particle precipitation near the magnetic poles. If the secondary and tertiary products of charged particle collisions with atmospheric molecules (including resultant ultraviolet emission) penetrate to the strato-

sphere, the effect on the chemistry may be direct, destroying molecular constituent (e.g., C_2H_6 with ~10 eV energy particles), or indirect by raising the local temperature through thermalization (as also suggested by Halthore *et al.* 1987). Direct excitation of molecular constituents is also possible, either by products of charged particle collisions or ultraviolet radiation resulting from auroral activity, leading to enhanced nonthermal emission. We investigated the possibility of the Io flux tube as a concentrated source for charged particles causing the observed infrared phenomena. However, a comparison of the interface of Io's flux tube with the atmosphere (J. E. P. Connerney 1986, private communication, NASA/Goddard Space Flight Center, Greenbelt, MD) failed to show any correlation with the hot-spot coordinates for the times of observation.

Some of these processes may be investigated in laboratory experiments. Products of charged particle and ultraviolet irradiation of a simulated Jovian stratospheric gas composition at appropriate temperatures and pressures should be studied to determine the end products. Preliminary work with corona discharge only has already been done (B. Khare 1985, private communication, Cornell University, Ithaca, NY), but must be pursued further to include the effects of incident charge particle beams and ultraviolet radiation as well.

SUMMARY

Our retrieved mole fractions of ethane on Jupiter are consistant with recent photochemical models (Yung and Strobel 1980, Gladstone 1983, Allen 1986). They are also in agreement with recent observational determinations within given error bounds (Maguire *et al.* 1985, Kim *et al.* 1985, Noll *et al.* 1986). Previous heterodyne observations on the south polar region (Kostiuk *et al.* 1983) yielded a lower C_2H_6 mole fraction using older molecular parameters. The precision of our retrieval is ±20%. The accuracy is based on the input parameters and the atmospheric model used. A twofold uncertainty is possible in the absolute C_2H_6 mole fractions retrieved based on reasonable changes in the atmospheric temperature profiles and altitude distribution of ethane. A comparison of our mean equatorial value of $2.8 \pm 0.6 \times 10^{-6}$ to previous results is given in Table II.

TABLE II

C_2H_6 mole fraction	Reference
3.6×10^{-4}	Ridgway (1974)
2.7×10^{-5}	Tokunaga *et al.* (1976)
2.7×10^{-6} (photochemical model, upper limit)	Yung and Strobel (1980)
$2.2\ (+1.8, -1.3) \times 10^{-6}$ (mesospheric)	Atreya *et al.* (1981)
$1.1\ (+1.1, -0.6) \times 10^{-6}$ (south pole)	Kostiuk *et al.* (1983)
$4 \pm 2.3 \times 10^{-6}$	Maguire *et al.* (1985)
$4.4 \pm 0.9 \times 10^{-6}$	Kim *et al.* (1985)
$4.9 \pm 1.3 \times 10^{-6}$	Noll *et al.* (1986)
$2.8 \pm 0.6 \times 10^{-6}$ (equatorial mean)	This work

A spatial map of Jovian stratospheric ethane indicates greater variability in emission and retrieved C_2H_6 mole fractions near the footprint of Io's flux tube and within the auroral regions. An increase in ethane emission and abundance is obtained near the south polar region. Within the north auroral oval at 180° long (System III, 1965) and 60° lat a significant decrease in ethane emission was observed in April 1983. This region coincides with the hot spot observed in 7.8 μm CH_4 emission and 13.6 μm C_2H_2 emission. Unlike the CH_4 emission, the behavior of ethane lines cannot be explained purely by a possible localized temperature increase. We suggest that a modification of stratospheric chemistry, forming more C_2H_2 at the expense of ethane, is responsible for the observed effects in the northern hot spot. Although dynamics may play a role in the lower stratosphere, ultraviolet hydrocarbon chemistry significantly modified by higher order effects of charged particles precipitating along the magnetic field

lines may be the best candidate process for generating the observed phenomenon.

ACKNOWLEDGMENTS

The authors thank Jim Faris, Jim Guthrie, and Howard Huffman for invaluable technical support. This work was supported by the NASA Planetary Astronomy Program.

REFERENCES

ATREYA, S. K. 1986. *Atmospheres and Ionospheres of the Outer Planets and Their Satellites*. Springer-Verlag, New York/Berlin.

ATREYA, S. K., T. M. DONAHUE, AND M. C. FESTOU 1981. Jupiter: Structure and composition of the upper atmosphere. *Astrophys. J.* **247,** L43–L47.

BEEBE, R. F., R. M. SUGGS, AND T. LITTLE 1986. Seasonal north–south asymmetry in solar radiation incident on Jupiter's atmosphere. *Icarus* **66,** 359–365.

CALDWELL, J., A. T. TOKUNAGA, AND F. C. GILLETT 1980. Possible infrared aurorae on Jupiter. *Icarus* **44,** 667–675.

CALDWELL, J., A. T. TOKUNAGA, AND G. ÖRTON 1983. Further observations of 8-μm polar brightenings of Jupiter. *Icarus* **53,** 133–140.

CALDWELL, J., H. HALTHORE, G. ORTON, AND J. BERGSTRALH 1987. Infrared polar brightenings on Jupiter. IV. Spatial properties of methane emission. Submitted for publication.

CLARKE, J. T., H. W. MOOS, S. K. ATREYA, AND A. L. LANE 1980. Observations from Earth orbit and variability of the polar aurora on Jupiter. *J. Astrophys.* **241,** L179–L182.

COMBES, M., TH. ENCRENAZ, L. VAPILLON, Y. ZEAU, AND C. LESQUEREN 1974. Confirmation of the identification of C_2H_2 and C_2H_6 in the Jovian atmosphere. *Astron. Astrophys.* **34,** 33–35.

CONNERNEY, J. E. P., M. H. ACUNA, AND N. F. NESS 1981. Modeling the Jovian current sheet and inner magnetosphere. *J. Geophys. Res.* **86,** 8370–8384.

DAUNT, S. J., A. K. ATAKAN, W. E. BLASS, G. W. HALSEY, D. E. JENNINGS, D. C. REUTER, J. SUSSKIND, AND J. W. BRAULT 1984. The 12 micron band of ethane: High-resolution laboratory analysis with candidate lines for infrared heterodyne searches. *Astrophys. J.* **280,** 921–936; also ATAKAN, A. K., W. E. BLASS, J. W. BRAULT, S. J. DAUNT, G. W. HALSEY, D. E. JENNINGS, D. C. REUTER, AND J. SUSSKIND (1983). *The 12 Micron Band of Ethane: A Spectral Catalog from 765 cm^{-1}–900 cm^{-1}*. NASA/GSFC Technical Memorandum 85108.

DROSSART, P., E. SERABYN, J. LACY, S. ATREYA, B. BEZARD, AND T. ENCRENAZ 1985. Acetylene, ethane and polar infrared brightening on Jupiter. *Bull. Amer. Astron. Soc.* **17,** 708.

DROSSART, P., B. BEZARD, S. ATREYA, J. LACY, E. SERABYN, A. TOKUNAGA, AND T. ENCRENAZ 1986. Enhanced acetylene emission near the north pole of Jupiter. *Icarus* **66,** 610–618.

GIERARSCH, P. J., B. J. CONRATH, AND J. A. MAGALHÃES 1986. Zonal mean properties of Jupiter's upper troposphere from Voyager infrared observations. *Icarus* **67,** 456–483.

GLADSTONE, G. R. 1983. *Radiative Transfer and Photochemistry in the Upper Atmosphere of Jupiter*. Ph.D. thesis, California Institute of Technology, Pasadena.

HALTHORE, R., A. BURROWS, AND J. CALDWELL 1987. Infrared polar brightenings on Jupiter. V. A thermal equilibrium model for the north polar hot spot. Submitted for publication.

HANEL, R. A., B. CONRATH, M. FLASAR, V. KUNDE, P. LOWMAN, W. MAGUIRE, J. PEARL, J. PIRRAGLIA, R. SAMUELSON, D. GAUTIER, P. GIERASCH, S. KUMAR, AND C. PONNAMPERUMA 1979a. Infrared observations of the Jovian system from Voyager 1. *Science* **204,** 972.

HANEL, R. A., B. CONRATH, M. FLASAR, L. HERATH, V. KUNDE, P. LOWMAN, W. MAGUIRE, J. PEARL, J. PIRRAGLIA, R. SAMUELSON, D. GAUTIER, P. GIERASCH, S. KUMAR, AND C. PONNAMPERUMA 1979b. Infrared observations of the Jovian system from Voyager 2. *Science* **206,** 952.

HILLMAN, J. J., G. W. HASLEY, AND D. E. JENNINGS 1985. Determination of temperature dependence of the H_2-broadening coefficient for ν_9 band of ethane: Implications for the outer planets. *Bull. Amer. Astron. Soc.* **17,** 707.

KIM, S. J., J. CALDWELL, A. R. RIVOLO, AND R. WAGENER 1985. Infrared polar brightening on Jupiter. III. Spectrometry from Voyager 1 IRIS experiment. *Icarus* **64,** 233–248.

KOSTIUK, T., AND M. J. MUMMA 1983. Remote sensing by IR heterodyne spectroscopy. *Appl. Opt.* **17,** 2644.

KOSTIUK, T., M. J. MUMMA, F. ESPENAK, D. DEMING, D. E. JENNINGS, W. MAGUIRE, AND D. ZIPOY 1983. Measurements of stratospheric ethane in the Jovian south polar region from infrared heterodyne spectroscopy of the ν_9 band near 12 microns. *Astrophys. J.* **265,** 564–569.

MAGUIRE, W. C., R. E. SAMUELSON, R. A. HANEL, AND V. G. KUNDE 1985. Latitudinal variation of acetylene and ethane in the Jovian atmosphere from Voyager IRIS observations. *Bull. Amer. Astron. Soc.* **17,** 708.

MONTGOMERY, C. G., J. M. SAARI, R. W. SHORTHILL, AND N. F. SIX, JR. 1966. *Directional Characteristics of Lunar Thermal Emission*. Boeing Document D1-82-0568, Technical Note R-213. Boeing Scientific Research Laboratories, Geo-Astrophysics Laboratory, Seattle, WA.

MUMMA, M. J., T. KOSTIUK, AND D. BUHL 1978. A 10

μm laser heterodyne spectrometer for remote detection of trace gases. *Opt. Eng.* **17,** 50.

NOLL, K. S., R. F. KNACKE, A. T. TOKUNAGA, J. H. LACY, S. BECK, AND E. SERABYN 1986. The abundances of ethane and acetylene in the atmospheres of Jupiter and Saturn. *Icarus* **65,** 257–263.

RIDGWAY, S. T. 1974. Jupiter: Identification of ethane and acetylene. *Astrophys. J.* **187,** L41–L43.

STROBEL, D. F. 1974. Hydrocarbon abundances in the Jovian atmosphere. *Astrophys. J.* **192,** L47.

SUSSKIND, J., D. REUTER, D. E. JENNINGS, S. J. DAUNT, W. E. BLASS, AND G. W. HALSEY 1982. Diode laser spectra of the torsional splitting in the ν_9 band of ethane: Torsion–vibration–rotation interactions and the barrier to internal rotation. *J. Chem. Phys.* **77,** 2728.

TOKUNAGA, A., R. F. KNACKE, AND T. OWEN 1976. Ethane and acetylene abundances in the Jovian atmosphere. *Astrophys. J.* **209,** 294–301.

TOKUNAGA, A. T., R. F. KNACKE, S. T. RIDGWAY, AND L. WALLACE 1979. High-resolution spectra of Jupiter in the 744–980 inverse centimeter spectral range. *Astrophys. J.* **232,** 603–615.

YUNG, Y. L., AND D. F. STROBEL 1980. Hydrocarbon photochemistry and Lyman alpha albedo of Jupiter. *Astrophys. J.* **239,** 395.